the label is represented as the smaller sphere of the dumbbell and the polymer coil as the larger one. The length of the dumbbell arm adjacent to the label is the sum of two contributions, d_0, describing the structure of the label, and a reorientational persistence length, p, which describes the section of the backbone participating in the reorientation of the label. The latter can be expected to be closely related to the length of Kuhn's equivalent segment of the polymer (p_K).

We now apply this model to demonstrate the consistency of the measurement of the local mobility (fluorescence depolarization) with the measurement of the polymer configuration (light scattering): In the present case the polymer is much larger than the label and its overall rotational mobility can be neglected. The rotational friction constant f of the attached label can be calculated (lever rule) to be

$$6\eta V_F \equiv f = 6\eta[\pi a(p + d_0)^2 + (4\pi/3)a^3] \quad (6)$$

where $(4\pi/3)\cdot a^3 = V_F(\text{free})$ is the equivalent rotational volume of the free label. The equivalent volumes V_F and V_F(free) are measured by time-resolved fluorescence depolarization and the parameter d_0 of FITC is known.[13] The persistence length p can thus be estimated by eq 6 to be 2 nm. An independent estimate of the length of the equivalent segment p_K can be obtained from light scattering data. It can be calculated from the radius of gyration R_G of the polymer in a θ solvent. Assuming this condition is fulfilled somewhere between 25% and 35% acetone (R_L = 7.3–6 nm) and estimating thus R_G to 11–9 nm (using $R_L = 0.67R_G$[19]), we obtain p_K = 2–1.4 nm. This value is in good agreement with the estimate from the fluorescence depolarization.

Combining the information from three independent methods, we have obtained a consistent picture of the polymer collapse in a poor solvent. The global mobility measured by dynamic light scattering and viscosimetry increase during the course of the transition into the compact state, while the local mobility of the backbone, as probed by the time-resolved fluorescence depolarization, decreases due to an increase of the internal friction.

Acknowledgment. We are indebted to Dr. P. Bigler for the NMR analysis, to Dr. D. G. Nealon for the HPLC results, to Dr. M. Borkovec for helpful comments. This work has been financially supported by the Swiss National Science Foundation.

References and Notes

(1) Nishio, I.; Sun, S.; Swislow, G.; Tanaka, T. *Nature (London)* **1979**, *281*, 208.
(2) Berne, B. J.; Pecora, R. *Dynamic Light Scattering*; Wiley: New York, 1976.
(3) See ref 2, p 187.
(4) Pusey, P. *Macromolecular Diffusion in Photon Correlation and Light Beating Spectroscopy*; Cummins, H. Z., Pike, E. R., Ed.; Plenum: New York, London 1973.
(5) Billingham, N. C. *Molar Mass Measurements in Polymer Science* Kogan Page: London, 1973; p 172 ff.
(6) O'Connor, D. V.; Phillips, D. *Time-Correlated Single Photon Counting*; Academic: London 1984.
(7) Patterson, P. M.; Jamieson, A. M. *Macromolecules* **1985**, *18*, 266.
(8) Chryssomallis, G.; Drickamer, H. G. *Chem. Phys. Lett.* **1979**, *67*, 381.
(9) Möller, F. "Amine durch Umlagerungsreaktionen", In *Methoden der Organischen Chemie*; Houben-Weyl, Thieme Verlag: Stuttgart, 1957; Bd XI/1, p 854.
(10) At the time of the study we were unaware of the method of Tanaka and Senju (Tanaka, H.; Senju, R. *Bull. Chem. Soc. Jpn.* **1976**, *49*, 2821) which appears to be better suited for polymers than the standard method in ref 9.
(11) Merki, P. Inaugural Dissertation der Universität Bern, Bern, Switzerland, 1984.
(12) Tschanz, H. P.; Binkert, Th. *J. Phys. E: Sci. Instrum.* **1976**, *9*, 1131.
(13) Rička, J.; Amsler, K.; Binkert, Th. *Biopolymers* **1983**, *22*, 1301.
(14) Rička, J. *Rev. Sci. Instrum.* **1981** *52*, 195.
(15) Leung, W. M.; Axelson, D. E.; Syme, D. *Colloid & Polym. Sci.* **1985** *263*, 812.
(16) Landau, F.; Zekhnini, Z.; Heatley, F. *Macromolecules* **1986**, *19*, 1895.
(17) Udenfriend, S.; Stein, S.; Böhlen, P.; Dairman, W.; Leimgruber, W.; Weigele, M. *Science (Washington, D.C.)* **1972**, *178*, 871.
(18) Molyneux, Ph. *Water-Soluble Synthetic Polymers I, II*; CRC Press: Boca Raton, FL, 1983.
(19) Tanford, C. *Physical Chemistry of Macromolecules*; Wiley: New York, 1961; p 345.
(20) Tanaka, T.; Fillmore, D.; Sun, S.; Nishio, I.; Swislow, G.; Shah, A. *Phys. Rev. Lett.* **1980** *45*, 1636.
(21) Viovy, J. L.; Monnerie, L. *Polymer* **1986**, *27*, 181.

Notes

Lattice Parameters and Packing Energies for Helical Polyacetylene

MARK L. ELERT*

Chemistry Department, U. S. Naval Academy, Annapolis, Maryland 21402

C. T. WHITE

Code 6129, Naval Research Laboratory, Washington, D.C. 20375. *Received August 15, 1986*

In 1983 Bates and Baker reported[1] the preparation of single crystals of polyacetylene (PA) from a solution of a polyacetylene–polystyrene block copolymer. Electron diffraction and X-ray analysis of the resulting PA crystals showed a hexagonal unit cell markedly different from the orthorhombic crystal structure of PA prepared by the usual Shirakawa technique.[2] To account for their data, Bates and Baker proposed that the PA chains prepared by their technique had crystallized in a helical conformation.

The existence of a helical isomer of polyacetylene is surprising, since conjugation of the π system is expected to favor a planar structure. Furthermore, the IR spectrum reported by Bates and Baker[1] appears to be a superposition of the spectra of polystyrene and planar *cis*-polyacetylene, whereas a recent calculation by Božović, Raković, and Gribov[3] shows that the IR spectra of helical and planar PA are expected to differ significantly. Because of the uncertainty in the experimental evidence in favor of the existence of helical PA, a number of theoretical investigations have been carried out during the past few years to elucidate the structure and stability of the proposed helical conformation.

We have previously reported[4,5] semiempirical MNDO calculations that indicate that planar *cis*-PA may indeed be unstable toward helix formation, with a unit cell length in the helix axis direction close to that reported by Bates

This article not subject to U.S. Copyright. Published 1987 by the American Chemical Society

and Baker.[1] Subsequently, ab initio calculations[6] on short PA chain segments with limited geometry optimization have also shown the helical isomer to be energetically stable. However, the energy changes associated with helix formation were found to be quite small (on the order of kT at room temperature) because of competition between two effects: energy increase in the helix due to loss of conjugation and energy lowering due to reduced 1,4 hydrogen–hydrogen nonbonded repulsion.[7]

Because the energy difference between isolated chains of planar and helical PA is so small, the stability of helical PA in the solid state might ultimately depend on the crystal packing energy of the helix relative to that of the planar isomer. In this paper we report calculations of the packing energy for helical PA in a hexagonal lattice using several standard intermolecular potential functions, compare our calculated optimal packing parameters to the experimental unit cell lengths reported by Bates and Baker[1], and consider the relative stability of helical and planar PA in the light of these results.

Chain Geometry

Bates and Baker[1] have reported on the basis of electron diffraction and X-ray scattering measurements that crystalline helical PA is composed of helices with six carbon atoms per helix turn, with a unit cell length of 4.84 Å. In a previous work[4] we showed on the basis of MNDO calculations that the lowest energy helix conformation satisfying these two constraints is defined by the following parameters: $R_1 = 1.47$ Å, $R_2 = 1.35$ Å, $\theta_C = 129°$, $\theta_H = 119°$, $\phi_1 = 102°$, and $\phi_2 = -2°$, where R_1 and R_2 are the C—C (single) and C=C (double) bond lengths, respectively, θ_C and θ_H are the C=C—C and C=C—H bond angles, and ϕ_1 and ϕ_2 are the dihedral angles for C=C—C=C and C—C=C—C. In these calculations the C–H bond length was constrained to have a value of 1.08 Å. The helix packing calculations reported here were done at this chain geometry. Additional calculations were performed at other geometries satisfying the experimental criteria (i.e., a unit cell length of 4.84 Å for a six-carbon helix turn) to verify that the packing parameters were insensitive to small changes in chain conformation.

Nonbonded Potentials

The Williams (IV) potential[8] has been widely used in the study of interchain interactions in polymers. It is especially suitable for PA because the parameterization of the Williams (IV) potential was obtained by fitting to the experimental crystal structures of both aliphatic and aromatic hydrocarbons. This potential has been used by Baughman et al.[9] to determine the packing energy and crystal structure of planar *cis*-polyacetylene.

The Williams potential is of the exp-6 type, i.e., it is of the form

$$V(r) = Ae^{-\alpha r} - Br^{-6}$$

To test for the possible dependence of the packing results on the particular form of the intermolecular potential chosen, we also performed calculations using two potential functions of the Lennard-Jones type for hydrocarbon polymers, proposed by Tai, Kobayashi, and Tadokoro.[10] (Tai et al. actually reported three sets of Lennard-Jones parameters for hydrocarbon polymer packing, but set I was optimized only for intrachain nonbonded interactions. We therefore report results only for sets II and III.) The parameters for the three potential functions W(IV), T(II), and T(III) are shown in Table I. The three sets lead to very different potential functions; for example, the minima in the H–H potential curves for T(II) and W(IV) occur at interatomic distances of 2.80 Å and 3.37 Å, respectively, and the well depth is 5 times deeper in the former case than in the latter. A graphical comparison of the potential curves corresponding to the parameter sets investigated here is presented in the paper of Tai et al.[10]

Table I
Intermolecular Potential Parameters Used in the Present Study (Energies in kcal/mol, Lengths in angstroms)

Williams (IV) $V(r) = Ae^{-\alpha r} - Br^{-6}$

	A	α	B
C–C	83630	3.60	568
C–H	8766	3.67	125
H–H	2654	3.74	27.3

Tai (II and III) $V(r) = Ar^{-12} - Br^{-6}$

	A (set II)	A (set III)	B (sets II and III)
C–C	558000	797000	370.0
C–H	82600	118000	128.0
H–H	11300	16100	46.8

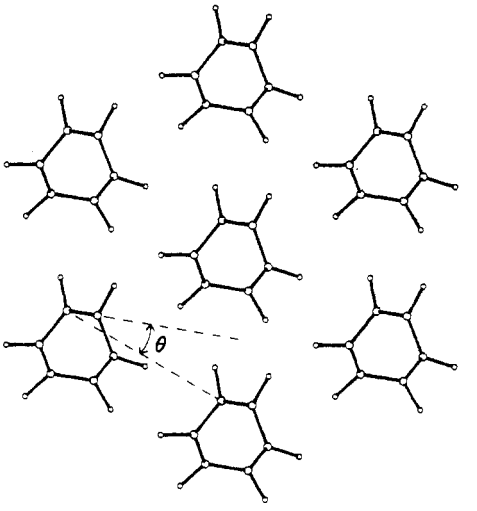

Figure 1. Projection of the helical polyacetylene lattice on a plane perpendicular to the helix axis. The lattice is shown in its equilibrium conformation as determined with the W(IV) potential. The definition of the setting angle θ is illustrated.

Packing Results

Helical polyacetylene chains were assumed to form a hexagonal lattice as determined by Bates and Baker.[1] The interchain potential energy was calculated as a function of the lattice unit cell parameter a and the setting angle of each chain within the unit cell. If one considers a projection of the lattice onto a plane perpendicular to the longitudinal helix axis as shown in Figure 1, then a corresponds to the distance between adjacent helix axes and the setting angle θ is the angle between a primitive axis vector of the unit cell and one of the edges of the distorted hexagonal projection of the helix.

The packing energy was calculated on a grid of 1° increments in setting angle and 0.01 Å in interchain distance. The equilibrium packing conformation reported here is simply the grid point of lowest energy with no further interpolation. A contour plot of packing energy vs. packing radius a and setting angle θ for the W(IV) potential (Figure 2) illustrates that the equilibrium conformation is well defined within the precision of the grid size employed.

The most stable packing arrangements as calculated from the three assumed interatomic potentials are shown in Table II. The optimum setting angle is essentially independent of the potential function chosen. The equilibrium interchain distance is somewhat larger for the T(II) and T(III) potentials than for W(IV), in spite of the

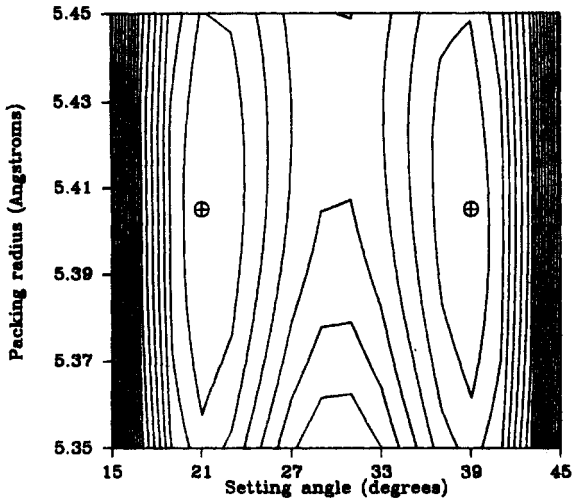

Figure 2. Contour plot of the packing energy for helical polyacetylene vs. packing radius a and setting angle θ using the W(IV) potential. Reflection symmetry about $\theta = 30°$ is apparent. The equilibrium conformation is indicated.

Table II
Unit Cell Parameters and Packing Energy (kcal/(mol of CH Units)) for Helical Polyacetylene in a Hexagonal Lattice, Using Three Different Intermolecular Potential Functions

	a, Å	θ, deg	packing energy
W(IV)	5.40	21	−1.238
T(II)	5.47	20	−1.114
T(III)	5.66	21	−0.884

Table III
Unit Cell Parameters and Packing Energy (kcal/(mol of CH Units)) for Planar Cis–Transoid Polyacetylene in an Orthorhombic Lattice, Using Three Different Intermolecular Potential Functions

	a, Å	c, Å	θ, deg	packing energy
W(IV) (this work)	7.30	4.30	52.5	−1.940
W(IV) (Baughman et al.[9])[a]	7.14	4.25	51.7	−1.675
T(II)	8.75	3.65	32.0	−1.626
T(III)	7.85	4.45	51.0	−1.247

[a] Included for comparison.

fact that the optimum H–H distance in the latter potential is larger. The differences in absolute packing energy are attributable mainly to the relative well depths of the C–C interaction potential curves.

We also performed packing optimization calculations for planar cis–transoid polyacetylene in its assumed orthorhombic crystal structure, using the intrachain geometry given by Baughman et al.[9] The results for the same three potential functions are shown in Table III, along with the results of Baughman et al. for the W(IV) potential. In the planar case there are two nonequivalent unit cell lengths a and c in the plane perpendicular to the chain axes, and the setting angle θ is taken as the angle between the ab plane and the plane of the polymer backbone. In contrast to the helical case, the minimum energy conformation for planar cis–transoid PA is difficult to locate precisely. As θ increases, the lattice can accommodate this change by increasing c and decreasing a with virtually no change in packing energy, so that the potential surface exhibits a long trough with an essentially flat bottom. The packing energy reported here is therefore quite accurate, whereas the unit cell conformation is simply one member of a large family of conformations whose energy is marginally lower than the others. For example, although the unit cell parameters reported in Table III for the T(II) surface appear to be abnormal, a local minimum at $a = 7.50$ Å, $c = 4.30$ Å, and $\theta = 52.0°$ has an energy only 0.033 kcal/mol higher than the conformation reported in Table III and is consistent with the results of the other potential functions reported there. We attribute the difference between Baughman's results[9] and ours for the W(IV) potential to slight differences in implementation of the cutoff radius, although both studies employ a nominal cutoff of 15 Å.

Discussion and Conclusions

Bates and Baker[1] have reported a unit cell parameter a (interchain distance) of 5.12 Å for helical polyacetylene based on their experimental results. All three of the potential functions employed in the present study predict larger chain separations, with the W(IV) potential being closest to the experimental value at 5.40 Å. The discrepancy can be attributed to the fact that our calculations are based on a rigid-chain model in which the geometry has been optimized for the *isolated* chain. Small adjustments to the chain conformation via low-energy bond bending could significantly increase the nonbonded H–H distance between adjacent helices and permit a closer packing of the chains.

In contrast, relaxation of the helix conformation in the presence of neighboring chains is not expected to significantly affect the setting angle of the helices. Particularly in view of the close agreement in predicted setting angle among the three potential functions tested and the strong curvature of the potential energy surface as a function of setting angle, we expect that this parameter is accurately predicted by the present study.

For each of the three sets of potential functions employed, the packing energy for planar polyacetylene is about 50% greater in magnitude than for the helical isomer. The predicted packing energy difference ranges from 0.36 kcal/(mol CH units) for T(III) to 0.70 kcal/(mol CH units) for W(IV). These results imply that the planar polyacetylene lattice is more stable than the helical lattice by an amount comparable to kT at room temperature. The energy difference could be even less than this if the rigid chains were allowed to relax in the lattice model.

Our previous MNDO calculations,[4,5] as well as the unrestricted Hartree–Fock calculations of Rao et al.,[6] showed that in isolated polyacetylene chains, the helical conformation was more stable than the planar cis form by approximately 0.6 kcal/(mol CH units). Apparently, however, interchain packing favors the planar conformation by about the same amount. This reinforces our earlier conclusion[4] that the conformation adopted by *cis*-polyacetylene in the solid state is governed by the preparation method (i.e., kinetic factors) rather than by thermodynamic considerations.

Acknowledgment. We thank David Deaven for help in performing the calculations. This work was supported by the NRL–USNA Cooperative Program for Scientific Interchange.

Registry No. PA, 25067-58-7.

References and Notes

(1) Bates, F. S.; Baker, G. L. *Macromolecules* **1983**, *16*, 1013.
(2) Shirakawa, H.; Ikeda, S. *Polym. J. (Tokyo)* **1971**, *2*, 231.
(3) Božovič, I.; Rakovič, D.; Gribov, L. A. *Phys. Rev. B: Condens. Matter* **1985**, *32*, 4286.
(4) Elert, M. L.; White, C. T. *Phys. Rev. B: Condens. Matter* **1983**, *28*, 7387.
(5) Elert, M. L.; White, C. T.; Mintmire, J. W. *Mol. Cryst. Liq. Cryst.* **1985**, *125*, 329.
(6) Rao, B. K.; Darsey, J. A.; Kestner, N. R. *Phys. Rev. B: Condens. Matter* **1985**, *31*, 1187.

(7) When hydrogen is replaced by fluorine in conjugated systems, steric effects are even more dramatic. A recent large-scale ab initio study [Dixon, D. A. *J. Phys. Chem.* **1986**, *90*, 2038] has shown that even in perfluoro-1,3-butadiene, where the chain is so short that 1,4 fluorine–fluorine repulsions are not present, 1,3 repulsions are sufficient to cause a nonplanar skew-*s*-*cis* conformation to be energetically favored.
(8) Williams, D. E. *J. Chem. Phys.* **1967**, *47*, 4680.
(9) (a) Baughman, R. H.; Hsu, S. L.; Pez, G. P.; Signorelli, A. J. *J. Chem. Phys.* **1978**, *68*, 5405. (b) Baughman, R. H.; Hsu, S. L. *J. Polym. Sci., Polym. Lett. Ed.* **1979**, *17*, 185.
(10) Tai, K.; Kobayashi, M.; Tadokoro, H. *J. Polym. Sci., Polym. Phys. Ed.* **1976**, *14*, 783.

Dye Labeling Technique for Monitoring the Cure of Polyimides and Polyureas: Model Compound Studies

R. J. MATHISEN, J. K. YOO, and C. S. P. SUNG*

Institute of Materials Science, Department of Chemistry, University of Connecticut, Storrs, Connecticut 06268.
Received September 22, 1986

Characterization of cross-linked polymers remains one of the challenging problems in polymer science. Our laboratory has been involved in developing new methods to probe cure reactions in network polymers. The approach we have taken is based on labeling by reactive dyes to mimic the curing agent and to use their photochemical and photophysical behavior to provide information on the curing process.

For example, we used a reactive label, *p,p'*-diaminoazobenzene (DAA) to monitor cure in epoxy–diamine resins. As the cure proceeds, λ_{max} of the $\pi \rightarrow \pi^*$ transition corresponding to the azo bond of DAA shows red-shifts (about 60 nm) in the visible spectra in a way that provides spectral discrimination for the cure products.[1] Furthermore, the fluorescence intensity of the DAA label at 560 nm increases sharply (more than 100 times), because of the fluorescence quantum yield of DAA increases more than a thousandfold when the amine groups of DAA become tertiary amines.[2] By analyzing visible and fluorescence spectra, we are able to obtain parameters characteristic of cure kinetics and mechanisms such as cure product composition, the reactivity ratio of primary and secondary amine, initial rate constants, and an activation energy of amine–epoxy reaction.[3,4] Finally, we compared experimental results with the theoretical predictions of Macosco and Miller on the weight average molecular weight and the soluble fractions.[4] In another epoxy–diamine system, we used *p,p'*-diaminostilbene as the reactive label, which showed red-shifts of only about 20 nm in the UV region.[5] Their fluorescence behavior was useful in correlating to the cure extent.

There is a tremendous interest in polyimides as high-temperature materials[6] and polyureas as new engineering materials.[7] In polyimides, the reaction of dianhydride with diamine first leads to the formation of amic acids followed by imidization. Cross-linking is often provided by acetylenic or norbonyl monomers. In polyureas, diisocyanate reacts with diamine to form ureas, whose secondary hydrogen can react further with isocyanate groups to form biuret-type cross-links.

In order to monitor the reaction products of these two polymers at various stages, we use a reactive label such as DAA to mimic the diamine component present in polyimide or polyurea synthesis. As the cure proceeds, the label shows spectral shifts in the UV–vis region corresponding to the various stages of the reaction. These shifts occur because of the distinctly different electronic states associated with each of the reaction products. Model compounds representing the various cure products have been synthesized and are shown in Scheme I.

Experimental Section

Solvents and Reagents. DAA was purchased from Eastman Kodak and recrystallized from methanol. Phthalic anhydride, dibutyltin dilaurate, and phenyl isocyanate were all purchased from Aldrich and used without further purification. *N*-methylpyrrolidone was purchased from Aldrich, distilled at reduced pressures, and stored over molecular sieve 4A. All other solvents were purchased from Aldrich and used without further purification.

Apparatus. Infrared spectra were recorded on a Nicolet 60SX FTIR spectrophotometer. UV–vis spectra were recorded on a Perkin-Elmer Lambda Array 3840 UV/vis spectrophotometer using NMP or Me_2SO as a solvent. Thermal analyses were carried out on a Omnitherm thermal analyzer with a DSC/DTA cell.

Synthesis. Model Diamic Acid. Diaminoazobenzene (0.50 g, 2.36 mmol) and phthalic anhydride (1.051 g, 7.08 mmol) were dissolved in 9 mL of glacial acetic acid, and the solution was stirred at room temperature for 1 h. The solution was poured into 25 mL of distilled water, and the yellow precipitate was collected by filtration. Recrystallization from ethanol yielded 0.887 g (74%) of diamic acid, mp 210–212 °C. The infrared spectra (KBr) showed absorptions at 3100 (νOH), 1665 (νC=O), 3278 (νNH), 1595 (νC=O), and 1541 cm^{-1} (νNH).

Model Amic Acid Imide. Aminonitroazobenzene (2.00 g, 8.27 mmol) and phthalic anhydride (1.94 g, 12.4 mmol) were refluxed in 50 mL of glacial acetic acid for 2 h, and the resulting precipitate was collected by filtration. The yellow solid was added to 40 mL of *N*-methylpyrrolidone and heated to reflux for 1 h. As the mixture cooled, fine crystals formed. These were collected and recrystallized from NMP to yield 1.99 g (64%) of imidonitroazobenzene (I).

The nitro group was reduced to an amine by refluxing I (0.60 g, 1.61 mmol) with $Na_2S{\cdot}9H_2O$(6.58 g, 27.4 mmol) in 25 mL of 80% methanol for 1 h. The methanol was removed under vacuum, and the yellow precipitate was collected by filtration and rinsed with small portions of cold water. The solid was recrystallized from water to yield 0.30 g (54%) of aminoimidoazobenzene (II).

Phthalic anhydride (0.130 g, 0.878 mmol) and II (0.200 g, 0.585 mmol) were dissolved in 5 mL of NMP and heated to about 50 °C for 4 h. The solution was cooled and upon addition of water a red precipitate formed. Recrystallization from methanol yielded 0.136 g (51%) of amic acid imide: m.p. 240–242 °C. The infrared spectra (KBr) showed absorptions at 3100 (νOH), 1665 (νC=O) 3278 (νNH), 1595 (νC=O), 1541 (νNH), and 1720 and 1770 cm^{-1} (νNC=O).

Model Diimide. Imidization was accomplished by dissolving the pure diamic acid (0.50 g, 0.98 mmol) in 20 mL of DMF and refluxing for 2 h. The golden brown precipitate was collected by filtration and recrystallized in DMF to yield 0.37 g (80%) of diimide: mp 360–362 °C. The infrared spectra (KBr) showed no amide absorption but imide absorption at 1720 and 1770 cm^{-1}.

Model Diurea. DAA (0.53 g, 2.50 mmol) and phenyl isocyanate (3.25 mL, 29.7 mmol) were dissolved in chlorobenzene and heated to 120 °C for 2 h under N_2 purge. The yellow precipitate was collected by filtration and recrystallized from Me_2SO/acetone to yield the diurea. The infrared spectra (KBr) showed absorptions at 3280 (νNH), 1635 (νC=O), 1590 (νNH), and 1540 cm^{-1} (νCNH).

Model Dibiuret. The diurea of DAA (0.45 g, 1.0 mmol) was dissolved in 25 mL of Me_2SO with dibutyltin dilaurate catalyst (25 mg, 0.04 mmol) and phenyl isocyanate (3.25 mL, 29.7 mmol). The solution was heated to 85 °C for 2 h and the excess phenyl isocyanate was removed under vacuum. Water was added, and the precipitated product was collected by filtration and dried. This crude compound was purified by column chromatography with an acetone/heptane mixture (4/5) to yield the dibiuret: mp 206 °C. The infrared spectra (KBr) showed absorptions at 3450 (νnH), 1635 (νC=O), 1590 (νNH), 1540 (νCNH), and 1690 cm^{-1} (ν biuret NC=O).

0024-9297/87/2220-1414$01.50/0 © 1987 American Chemical Society